

RESEARCH

Open Access



# Genomic DNA methylation profile in peripheral blood of children with congenital biliary dilatation

Chenyao Wang<sup>1†</sup>, Yuelan Zheng<sup>1†</sup>, Yan Wang<sup>1</sup> and Qi Feng<sup>1\*</sup>

## Abstract

**Background** Congenital biliary dilatation (CBD) is a prevalent congenital biliary disease in children, particularly in Asian populations, yet its etiology remains poorly understood. This study aimed to investigate the genome-wide DNA methylation profile in the peripheral blood of children with CBD to identify potential epigenetic mechanisms involved in its pathogenesis.

**Methods** Genome-wide DNA methylation profiles were compared between whole blood samples from 37 children with CBD and 24 healthy controls using the Illumina Infinium Human MethylationEPIC (850 K) BeadChip. Bioinformatic analyses were performed to identify differentially methylated positions (DMPs) and regions (DMRs), and functional enrichment analysis was conducted on associated genes.

**Results** We identified 24,230 differentially methylated sites associated with 5,863 genes. Among these, 8,313 sites were hypermethylated and 15,917 were hypomethylated in CBD patients compared to controls. 54 significant differentially methylated regions (DMRs) were also detected. Functional enrichment analysis revealed that the differentially methylated genes were significantly enriched in key biological pathways, most notably the T cell receptor signaling pathway.

**Conclusion** This study presents the first comprehensive analysis of genome-wide DNA methylation in CBD, revealing significant epigenetic alterations in peripheral blood. These findings suggest that aberrant DNA methylation, particularly in genes regulating immune pathways, may play a critical role in the development of CBD and could provide valuable insights for identifying novel diagnostic biomarkers.

**Keywords** Congenital biliary dilatation, DNA methylation, Epigenetics, Differentially methylated regions (DMRs)

<sup>†</sup>Chenyao Wang and Yuelan Zheng contributed equally to this work.

\*Correspondence:

Qi Feng

benjaminfeng@126.com

<sup>1</sup>Department of Hepatobiliary Tumor Surgery, Shen Zhen Children's Hospital, Shenzhen, Guangdong, China



## Background

Congenital biliary dilatation (CBD) is a relatively rare biliary tract disease [1]. In contrast to the incidence observed in Europeans and Americans, the incidence of CBD is much higher in Asia, particularly among Asian populations, where it can be as high as 1/1,000 [2]. The current reason for the high incidence among Asians remains unclear. CBD mainly affects infants and children, with a higher proportion in females, and the incidence ratio of male to female is about 1:4 [3]. The widely recognized pathogenesis involves congenital biliary maljunction. The dilated bile ducts cause dilatation-stenosis-like biliary stricture, which subsequently leads to the abnormality of bile dynamics, causing cholestasis and then inducing biliary tract inflammation [4, 5]. At present, the generally accepted surgical method is complete cyst resection and hepatic duct jejunal anastomosis [6]. However, it may increase life-threatening risks when undergoing operation at childhood [7]. Currently, the lack of effective biomarkers for early diagnosis of CBD greatly limits the treatment of CBD [8]. Therefore, screening effective biomarkers is crucial for the early diagnosis.

DNA methylation represents a significant epigenetic modification that can influence the expression and alternative splicing of genes, thereby maintaining genome stability [9, 10]. Nowadays, many researchers have reported that aberrant DNA methylation plays a critical role in the occurrence and development of a range of congenital diseases by regulating the abnormally methylated loci in patients [11, 12]. Nevertheless, there is a paucity of research investigating the occurrence of aberrant DNA methylation in patients with CBD. Mori H et al. [8] demonstrated that Biliary tract cancer may develop later in children with CBD and adults with maljunction, potentially mediated through histone deacetylase (HDAC) and activation-induced cytidine deaminase (AID) expression via epigenetic and genetic mechanisms [8]. Wanvisa Udomsinprasert et al. [13] demonstrated a positive correlation between Alu and LINE-1 methylation and relative telomere length in patients with biliary atresia (BA), indicating that retrotransposon hypomethylation is associated with plasma 8-OHdG in BA patients. However, the role of DNA methylation in the underlying mechanisms of CBD remains unclear.

In this study, we first evaluated the genome-wide DNA methylation characteristics of CBD through the Illumina Infinium Human Methylation 850 k BeadChip. To investigate the DNA methylation patterns in children with CBD and a control group, we performed a comparative analysis of the genome-wide DNA methylation profiles of whole blood samples from patients with CBD and a control group. Moreover, this is the first study to investigate genome-wide epigenetic landscapes of congenital bile duct dilatation in children, thereby elucidating the potential epigenetic differences associated with CBD.

## Methods

### Study objectives

This case-control study recruited consecutive patients with CBD diagnosed at the Shenzhen Children's Hospital, between March 2020 and March 2021. In order to be eligible for inclusion in the study, participants had to meet the following criteria: a confirmed diagnosis of CBD, as determined by computed tomography (CT) and/or magnetic resonance imaging (MRI), and the provision of informed consent in writing. The control subjects exhibited no symptoms or history of hepatobiliary disease. Finally, 37 patients and 24 controls were enrolled in the study following the procurement of written informed consent from all subjects. All research protocols were approved by the Ethics Committee of Shenzhen Children's Hospital (No.202002902) according to the State Drug Administration and the National Health and Wellness Commission's Code for Quality Management of Drug Clinical Trials (2020), Code for Quality Management of Clinical Trials of Medical Devices (2016), the Ministry of Health's "Biomedical Research Involving Humans Ethical Review Measures (2016), the Declaration of Helsinki, and the CIOMS Ethical Principles for Medical Research Involving Human Subjects.

Gender, age, systolic blood pressure (SBP), diastolic blood pressure (DBP), Triglycerides (TG), Total Cholesterol (TC), Alanine aminotransferase (ALT), total bilirubin (TBil) and  $\gamma$ -glutamyl transferase (GGT) were all recorded at the time of admission.

### Illumina Infinium Human Methylation 850 K bead chip

DNA from whole blood of patients and controls was meticulously extracted using a reagent kit sourced from Yeasen (China), in strict compliance with the manufacturer's protocol. The DNA samples' purity and yield were determined using a Thermo Scientific NanoDrop 2000, ensuring the quality for subsequent analysis. For the conversion to bisulfite-modified DNA, 500 ng of each genomic DNA sample was processed with the EZ DNA Methylation-Gold Kit (Zymo Research, USA), following the manufacturer's instructions. Employing the Illumina Human Methylation 850 K BeadChip (LC Sciences, Hangzhou, China), we conducted a thorough analysis of methylation patterns. The platform's probes and hybridization conditions were tailored to the bisulfite-modified sequences, with the resultant fluorescence intensity ratios providing a direct measure of methylation status. Our dataset has been uploaded to the NCBI Gene Expression Omnibus (GEO) database. The project accession number is GSE275555, and the data can be accessed at the following link: <https://www.ncbi.nlm.nih.gov/geo/query/acc.cgi?acc=GSE275555>.

**Table 1** Characteristics of cases and controls

|                                  | CBD(n=37)     | Healthy controls(n=24) | P         |
|----------------------------------|---------------|------------------------|-----------|
| Age(months)                      | 40.28 ± 4.506 | 40.10 ± 6.220          | P=0.8962  |
| Sex(M/F)                         | 18/19         | 11/13                  | P>0.9999  |
| Alanine aminotransferase (U/L)   | 27.97 ± 16.86 | 18.210 ± 9.51          | P=0.0125* |
| Aspartate aminotransferase (U/L) | 61.42 ± 8.997 | 28.57 ± 11.543         | P<0.0001  |
| Total bilirubin (μmol/L)         | 20.78 ± 9.230 | 8.732 ± 2.999          | P<0.0001  |

Data are presented as mean ± SD or number. P < 0.05 CBD vs. Healthy controls

### DNA methylation quality control and processing

The IDAT files from the array data were processed using the ChAMP package (version 3.20) in R (version 3.3.3). Samples were excluded if they had a Failed CpG Fraction exceeding 0.10. Probes were excluded based on a *p*-value

threshold of 0.01, mapping ambiguity, non-CpG status, or insufficient bead counts in over 5% of the samples. The raw data are available in Additional file 1:Table S1. Methylation status for all probes was quantified as  $\Delta\beta$  values, calculated as the ratio of methylated probe intensity to the total probe intensity. A probe was classified as hypermethylated if its mean  $\Delta\beta$  value in the CBD cases was greater than the control mean by at least 0.2, and as hypomethylated if its mean  $\Delta\beta$  value in the CBD cases was less than the control mean by at least -0.2.

### Bioinformatic analysis

Microarray raw data from the Illumina Infinium Human Methylation 850 K BeadChip were subjected to a comprehensive pre-processing workflow using the R minfi package [14] (Version 1.42.0). This workflow included

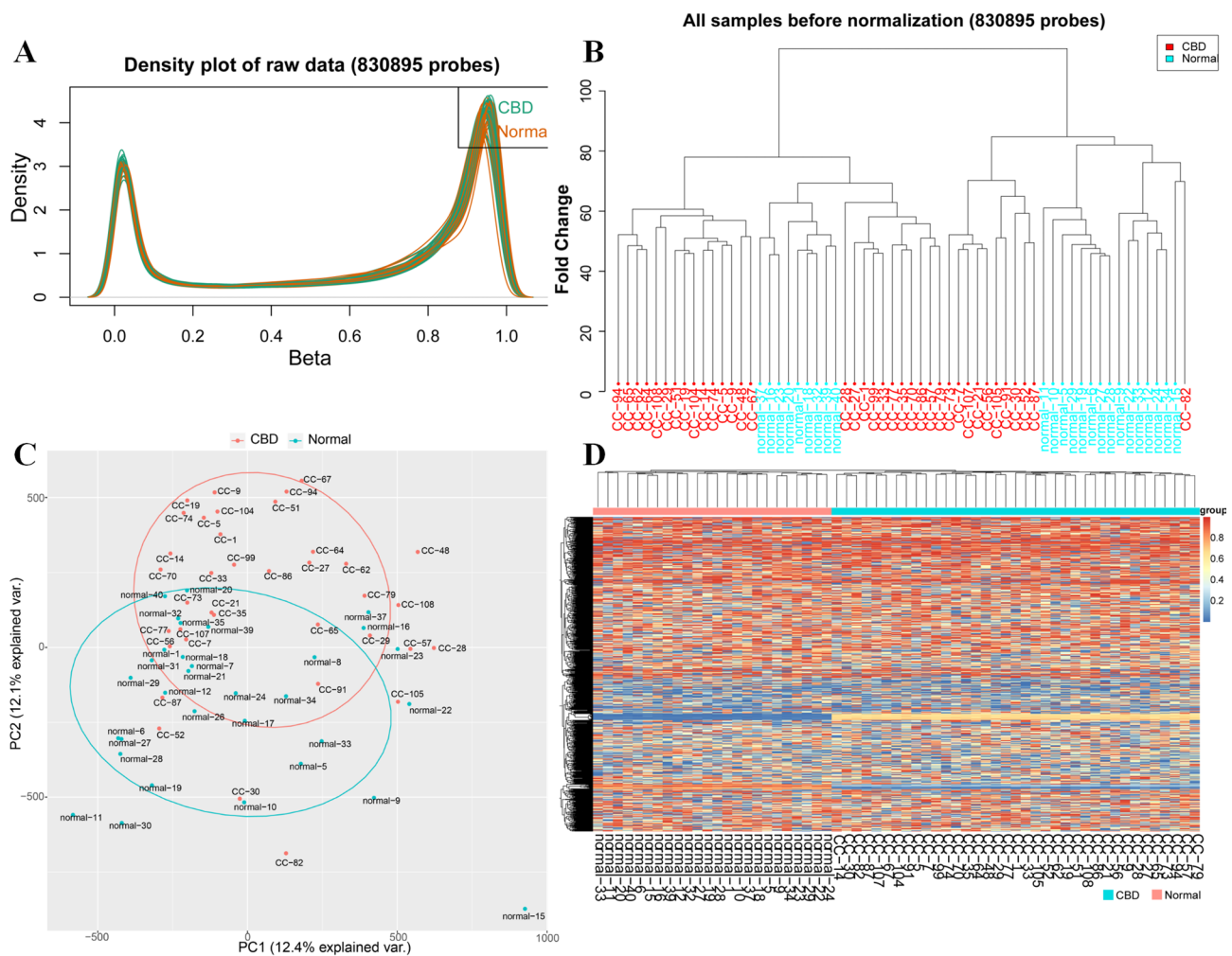


**Fig. 1** Density plot and principal component analysis (PCA) plot. **A** Density plot. This plot illustrates the distribution of  $\beta$  values representing methylation levels for the 37 CBD patients (depicted in green) and the 27 healthy controls (depicted in orange). **B** Raw Sample Cluster plot before normalization (830,895 probes). **C** PCA plot based on all CpG sites. No discernible separation is observed between the CBD patients (red dots) and the healthy controls (blue dots). PC1 explains 12.4% variance, and PC2 explains 12.1% variance. **D** Heatmap displaying methylation differences across 24,230 DMPs. Each row represents a DMP, and each column represents a subject. Red indicates hypermethylation in CBD patients compared to controls, while blue indicates hypomethylation



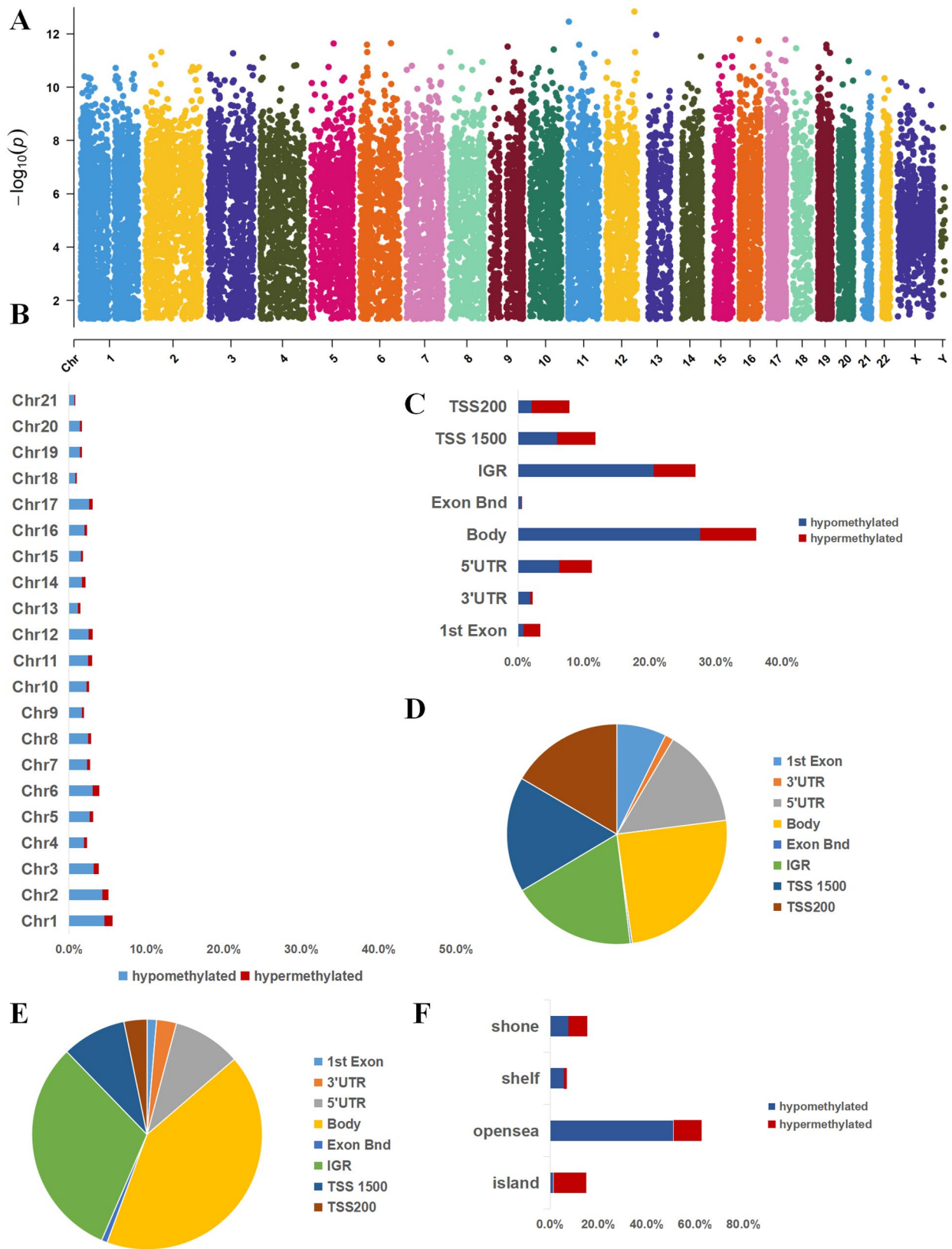


**Fig. 3** (See legend on next page.)

(See figure on previous page.)

**Fig. 3** Distribution of methylation sites in the chromosomes and functional analysis of DMPs. **A** Distribution of 24,230 DMPs across chromosomes, with hypermethylation in red and hypomethylation in blue. **B** Distribution of DMPs along the chromosome, showing the percentage of hypermethylated (red) and hypomethylated (blue) sites. **C** The distribution percentages of the 24,230 DMPs across different gene regions, including gene body, TSS1500, TSS200, 3'UTR, 5'UTR, 1st Exon and intergenic regions (IGR). Red bars represent hypermethylated DMPs, whereas blue bars represent hypomethylated DMPs. **D** The distribution of hypermethylation sites. **E** The distribution of hypomethylation sites. **F** The distribution percentages of the 439 DMPs in different CpG island regions, including Shore, Shelf, CpG island and Open Sea

and batch effects. DMPs were defined by a  $|\Delta\beta|$  threshold of  $\geq 0.20$  and a Holm-adjusted  $p$  value  $\leq 0.05$ , while identified as clusters of probes within a 2000 bp window, exhibiting consistent methylation changes and meeting the same statistical significance criteria [17]. The Probe Lasso method was applied for DMR analysis. Functional annotation of genes within DMRs was conducted using the Kobas tool [18] (Version 3.0) (<http://kobas.cbi.pku.edu.cn/kobas3>), accessible at Kobas. Enrichment analysis for Gene Ontology and Kyoto Encyclopedia of Genes and Genomes (KEGG) pathways was performed, with a false discovery rate  $< 0.05$  deemed significant.

#### Pyrosequencing analysis

DNA was subjected to bisulfite conversion using the EZ DNA Methylation-Gold Kit (ZYMO Research) following the manufacturer's guidelines, post-extraction. The converted DNA was then amplified via PCR with the TaKaRa EpiTaq HS Kit (TaKaRa) in a 50  $\mu$ L reaction, incorporating 20 pmol/L sequencing primer and 50 ng of bisulfite-converted DNA. PCR products, after agarose Gel purification, were pyrosequenced with the PyroMark Gold Q96 system (Qiagen), according to the provided protocol. PyroMark Q96 software (v2.5.8, Qiagen) was utilized for data acquisition and analysis.

#### Quantitative real-time PCR

For RNA analysis, total RNA was isolated using TRIzol reagent, and cDNA was synthesized with the Promega GoScript Reverse Transcription Mix. mRNA levels were assessed via quantitative real-time PCR (qRT-PCR) employing the GoTaq qPCR Master Mix (Promega) on an ABI StepOnePlus system. The  $2^{-\Delta\Delta C_t}$  method was applied to determine relative gene expression levels, with experiments conducted in triplicate. Primer sequences are detailed in Additional file 1: Table S2.

#### Statistical analysis

To investigate the phenotypic differences between the CBD patients and healthy controls, we utilized a series of statistical tests. Continuous variables were compared using the Student's  $t$ -test, assuming normal distribution, while the Mann-Whitney U test was employed for non-normally distributed data. Categorical variables were analyzed using the Chi-square test. A two-tailed  $p$ -value of less than 0.05 was considered statistically significant. All statistical analyses were conducted using Graphpad prism8.0.

## Results

### Blood genomic DNA methylation variations in CBD patients

In this study, we enrolled 61 individuals, including 37 children diagnosed with Congenital Biliary Dilatation (CBD) (aged  $40.28 \pm 4.506$  months) and 24 age- and sex-matched healthy controls (aged  $40.10 \pm 6.220$  months). A comprehensive set of demographic, clinical, and laboratory data for these participants is presented in Table 1. There were no significant differences in age or gender between CBD patients and healthy controls. However, CBD patients had significantly higher levels of liver enzymes, such as ALT ( $P < 0.05$ ), AST ( $P < 0.001$ ) and TBil ( $P < 0.001$ ).

We performed a genome-wide DNA methylation analysis using the Illumina Infinium Human Methylation 850 k BeadChip, analyzing 830,895 CpG sites. After quality control and normalization, methylation levels were compared between 37 CBD cases and 24 controls, applying a stringent threshold of  $\text{adj}P\text{Val} < 0.05$  (BH-adjusted) and  $|\Delta\beta| > 0.10$ . The density plot indicated that the methylation levels in the samples from patients with CBD and healthy controls were relatively similar (Fig. 1A, B). Differentially methylated sites are reported with  $\beta$ -values. Principal component analysis (PCA) on the 832,347 CpG sites did not fully separate CBD patients from controls (Fig. 1C). The analysis identified 24,230 differentially methylated sites ( $\text{adj}P$  value  $< 0.05$ ), which were mapped to 5,863 genes (Fig. 1D).

### CBD-associated site-specific differences in DNA methylation

This study presents a comparative epigenomic analysis between CBD patients and controls, focusing on DNA methylation differences. Utilizing the Illumina Human Methylation 850 K Beadchip, we identified 24,230 differentially methylated positions (DMPs) with statistically significant methylation variance in CBD cases (corrected  $P < 0.05$ ). Figure 2A displays a Manhattan plot of the top DMPs associated with CBD. Of these, 8,313 (34.31%) showed hypermethylation ( $\text{adj}P\text{Val} < 0.05$ ,  $\Delta\beta > 0.10$ ), and 15,917 (65.69%) displayed hypomethylation ( $\text{adj}P\text{Val} < 0.05$ ,  $\Delta\beta < 0.10$ ) (Fig. 2B). The results indicate that the majority of the significantly differentially methylated sites in children with CBD were identified within the gene body area. Furthermore, the distribution of hypomethylation and hypermethylation

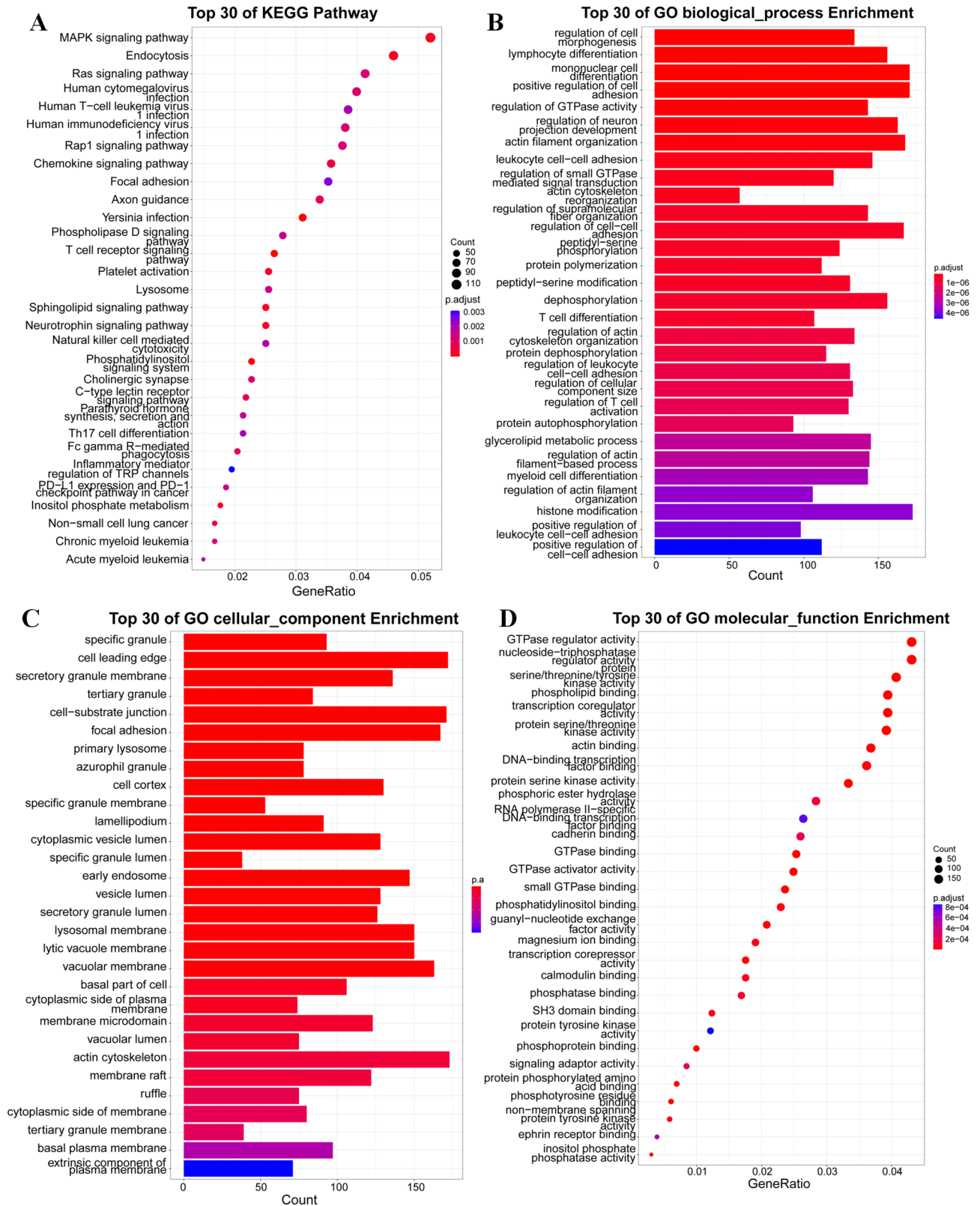


**Fig. 4** Ontological and Functional Enrichment Analysis of Differentially Methylated Genes. **A** Top 30 KEGG pathway enrichment. **B** Top 30 Gene Ontology Biological Process Enrichment. **C** Top 30 Gene Ontology Cellular Component Enrichment. **D** Top 30 Gene Ontology Molecular Function Enrichment. The vertical axis indicates the name of the KEGG pathway or GO category, the horizontal axis represents the enrichment factor, and the size of the circle indicates the number of differential methylation-related genes involved in the pathway or category

**Table 2** Top 30 Differentially methylated region (DMR) between CBD cases and the control group

| DMR    | Gene  | dmrRank | CHR | dmrSize | dmrCoreStart | dmrCoreEnd | dmrCoreSize |
|--------|---|---------|-----|---------|--------------|------------|-------------|
| DMR_1  | PEX10   | 23      | 1   | 174     | 2345333      | 2345475    | 143         |
| DMR_6  | DUSP6   | 28      | 12  | 316     | 89744471     | 89744701   | 231         |
| DMR_7  | GOLGA3  | 41      | 12  | 3518    | 133343405    | 133346306  | 2902        |
| DMR_8  | HTR2A   | 26      | 13  | 220     | 47472140     | 47472349   | 210         |
| DMR_9  | CEBPE   | 31      | 14  | 4192    | 23586582     | 23588616   | 2035        |
| DMR_10 | LOC404266;HOXB6                                   | 37      | 17  | 1864    | 46681111     | 46682319   | 1209        |
| DMR_11 | TMEM49;MIR21                                      | 33      | 17  | 4192    | 57915665     | 57918682   | 3018        |
| DMR_12 | LOC100130933;RECQL5                               | 48      | 17  | 4192    | 73641809     | 73643683   | 1875        |
| DMR_13 | SLC16A3   | 46      | 17  | 3518    | 80196719     | 80199608   | 2890        |
| DMR_14 | C18orf1   | 27      | 18  | 967     | 13611370     | 13611824   | 455         |
| DMR_15 | FXYD1   | 54      | 19  | 3531    | 35629022     | 35630474   | 1453        |
| DMR_16 | RPL13AP5;SNORD33;SNORD35A;SNORD34;RPL13A;SNORD32A | 35      | 19  | 2096    | 49993125     | 49994485   | 1361        |
| DMR_17 | SNORD12B;C20orf199;MIR1259;SNORD12                | 49      | 20  | 1917    | 47896448     | 47897451   | 1004        |
| DMR_18 | NFAM1   | 29      | 22  | 878     | 42828125     | 42828516   | 392         |
| DMR_19 | STAB1   | 32      | 3   | 878     | 52529085     | 52529524   | 440         |
| DMR_2  | NDUFS2;FCER1G                                     | 24      | 1   | 4250    | 161183762    | 161185092  | 1331        |
| DMR_20 | NA  | 25      | 6   | 604     | 28601271     | 28601519   | 249         |
| DMR_21 | TRIM39  | 52      | 6   | 2631    | 30296689     | 30298768   | 2080        |
| DMR_22 | HLA-E   | 19      | 6   | 2276    | 30459317     | 30460798   | 1482        |
| DMR_23 | DDR1  | 44      | 6   | 910     | 30860130     | 30860960   | 831         |
| DMR_24 | HLA-B   | 39      | 6   | 3518    | 31321433     | 31322996   | 1564        |
| DMR_25 | LTA;TNF   | 45      | 6   | 4192    | 31539973     | 31543686   | 3714        |
| DMR_26 | SNORA38;BAT2                                      | 53      | 6   | 1866    | 31590513     | 31592247   | 1735        |
| DMR_27 | VAR5  | 43      | 6   | 525     | 31762409     | 31762901   | 493         |
| DMR_28 | NEU1;SLC44A4                                      | 50      | 6   | 2819    | 31832173     | 31834178   | 2006        |
| DMR_29 | ATF6B   | 38      | 6   | 1313    | 32086425     | 32087190   | 766         |
| DMR_3  | C10orf26  | 34      | 10  | 940     | 104535521    | 104536121  | 601         |
| DMR_30 | PBX2;GPSM3  | 47      | 6   | 5265    | 32157150     | 32161747   | 4598        |

sites in comparison to all probes on the 850 k Illumina array revealed no significant difference (Fig. 2C and D). The 24,230 DMPs with annotated biological functions were mapped to 5,863 distinct genes (Additional file 1:Table S3). Figure 2E illustrates the top 70 genes with the most pronounced differential methylation.

The differentially methylated sites were distributed across all chromosomes (Fig. 3A and B). A detailed examination of hypermethylated sites revealed the following distribution across functional genomic domains: 1,529 (18.39%) in noncoding regions, 2,789 (33.55%) at transcription start sites, 2,061 (24.79%) in coding regions and 104 (1.25%) within the 3' untranslated region (UTR) termini (Fig. 3C and D). Hypomethylated sites were distributed as follows: 4981(31.29%) in noncoding intergenic regions, 6679(41.96%) in coding regions, 1950(12.25%) at transcription start sites, and 446 (2.8%) were in the end of a 3' UTR (Fig. 3C and E)). Among methylation sites in promoter regions, 3624 were located in a CpG island, 3709 were in a shore, 15,211 were in an opensea, 1686 in shelf (Fig. 3F).

#### Ontology functional analysis of differentially methylated genes in the blood of patients with CBD

The dataset encompassing 24,230 biologically annotated sites was mapped to 5,863 distinct genes. A gene biological process analysis (Bonferroni corrected  $p$ -value < 0.05) revealed significant enrichment of these differentially methylated genes (DMGs) in processes such as metabolic regulation, cell signaling, and the catabolism and metabolism of cellular and intracellular compounds, as well as the regulation of stimuli from both endogenous and exogenous sources (Fig. 4A, B). Cellular component analysis (Bonferroni corrected  $p$ -value < 0.05) indicated a notable enrichment of these genes within intracellular compartments, particularly at cell-substrate junctions and the leading edges of cells (Fig. 4C). Molecular function analysis (Bonferroni corrected  $p$ -value < 0.05) of DMGs showed significantly enrichment in the T cell receptor signaling pathway, Phosphatidylinositol signaling system, Inositol phosphate metabolism and Endocytosis (Fig. 4D). The gene ontology enrichment analyses, focusing on the three aforementioned categories, highlighted the top 10 most significant  $p$ -values for each.

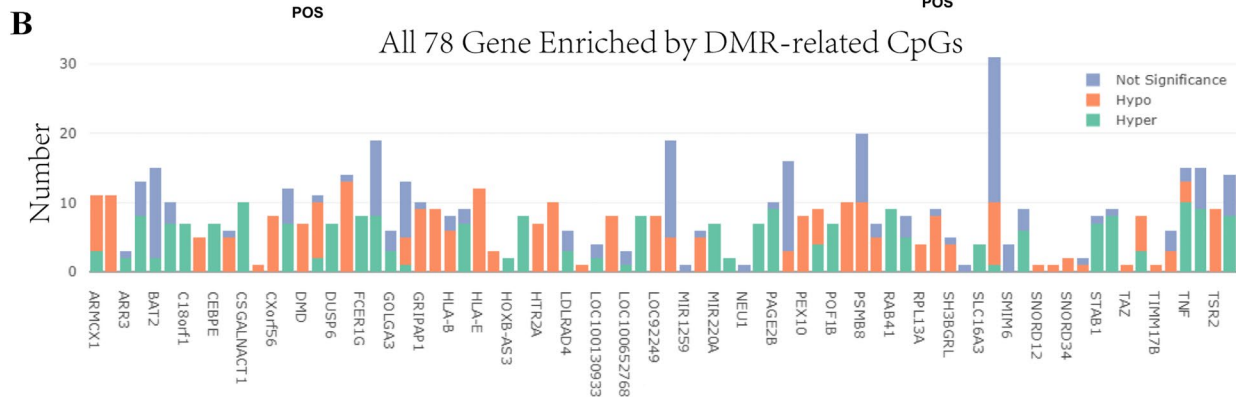
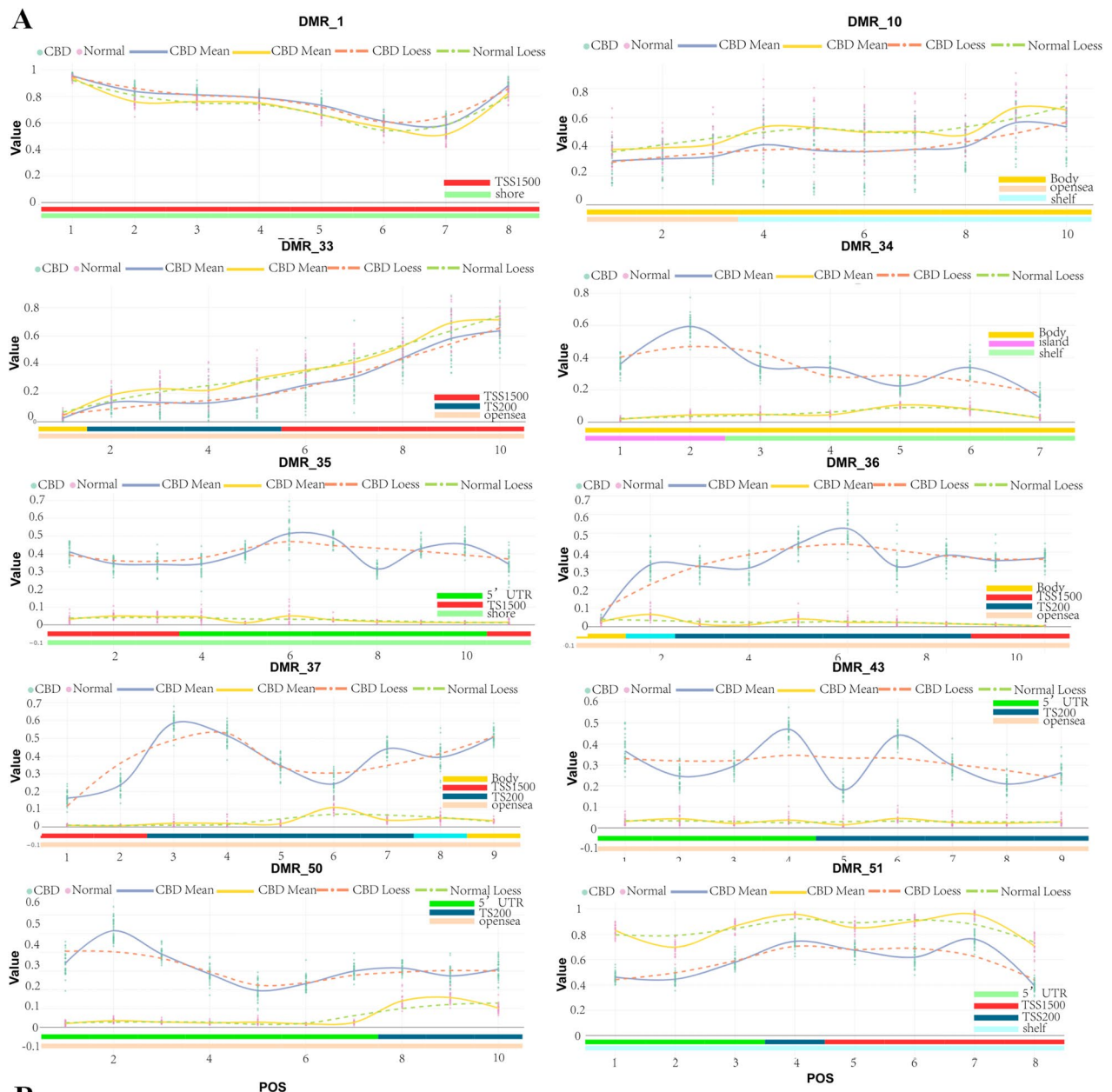


Fig. 5 (See legend on next page.)

(See figure on previous page.)

**Fig. 5** DMR (differentially methylated region) analysis. **A** Differentially methylated regions (DMR\_1, DMR\_34, DMR\_35, DMR\_36, DMR\_37, DMR\_43 and DMR\_50) demonstrate that the expression of these genes in CBD cases is apparently higher than in the control group; DMR\_10, DMR\_33 and DMR\_51 are hypomethylated between CBD cases and the control group. (method = "ProbeLasso"; minProbes = 7; adjPvalDmr < 0.05 (adjust.method = "BH") mean LassoRadius = 375; minDmrSep = 1000, minDmrSize = 50, adjPvalProbe < 0.05.) **B** The bar chart shows that TOP 78 hyper-enriched gene by DMR-related CpGs among all 5,863 genes

### Functional analysis of DMRs of differentially methylated genes in the blood of patients with CBD

According to the differential methylation region (DMR) analysis, we found that 54 DMR between CBD cases and the control group showed a significant difference (DMR\_1 ~ DMR\_54, Table 2, Additional file 1: Table S4). As is shown in Fig. 5A and Table 2, DMR\_1, DMR\_34-37, DMR\_43 and DMR\_50 were hypermethylated between CBD cases and the control group, while DMR\_10, DMR\_33 and DMR\_51 were hypomethylated. Notably, DMR\_1 in the PEX10 gene demonstrate a marked difference, with higher methylation values in the CBD group. Among the differentially methylated positions sites, cg13306335, cg14373988, cg20136951, cg20823695, cg24439334, cg20664247, cg23626733 and cg23629166 was hypermethylated in TSS1500 and shore region (Fig. 5A). DMDCSGALNACT1 gene, present in DMR\_33, had DMPs cg15379858, cg11155735, cg23328404, cg02694058, cg11505841, cg14818701, cg18325192, cg20450123, cg14854503 and cg24423468 hypomethylated in the transcription start site and open sea region. In total, DMR\_1 to DMR\_54 encompassed 489 differentially methylated positions related to 78 genes (Fig. 5B).

### Pyrosequencing validation and qRT-PCR validation

To explore the mechanisms underlying methylation alterations, we identified a set of genes involved in methylation regulation, MAP kinase inactivation, and inflammatory signaling pathways, including CEBPE, DUSP9, POF1B, OTUD5, WDR45, and XIAP. Six CpG sites within these genes showed the most significant methylation differences across the dataset. Methylation profiles of CpG sites in DUSP9, POF1B, and WDR45 varied markedly among the different groups (Fig. 6A). To further assess the functional relevance of these genes in CBD, we compared their mRNA expression levels between CBD patients and controls. Our results revealed significant expression divergences, in the expression of these genes between CBD patient samples and control samples (Fig. 6B). Our results revealed significant expression divergences, corroborating the methylation array data and suggesting a potential link between methylation status and gene expression in CBD pathophysiology.

### Discussion

Genome-wide DNA methylation is a critical and important mechanism in the field of epigenetics [13]. To our knowledge, this study is the first comprehensive analysis

to reveal a distinct genome-wide DNA methylation profile in the whole blood of CBD patients. A total of 24,230 DMPs and 54 DMRs were identified between the CBD and control groups. The significantly enriched KEGG pathways of the DMPs included T cell receptor signaling pathway, Phosphatidylinositol signaling system, Inositol phosphate metabolism, Endocytosis and MAPK signaling pathway. GO analysis revealed DMPs were significantly enriched in the regulation of specific regulation of cell morphogenesis, lymphocyte differentiation, positive regulation of cell adhesion and regulation of GTPase activity. Among these 54 DMRs, 7 DMRs were hypermethylated and 3 (DMR\_10, DMR\_33 and DMR\_51) were hypomethylated in CBD cases. Pyrosequencing and qPCR validation confirmed the differential methylation and expression of key genes including CEBPE, DUSP9, POF1B and WDR45. Overall, our analysis suggests that changes in DNA methylation patterns might influence the development of CBD.

CCAAT/enhancer binding proteins (CEBPs) are significant transcription factors that regulate cell differentiation and proliferation [19, 20]. Ewa Musialik et al. [21] reported high methylation levels at CEBPE promoter in AML patients, suggesting that DNA methylation of CEBPE plays a critical role in diseases. Dual-specificity phosphatase 9 (DUSP9) is a strong negative regulator of transcription factor activating MAPK pathways [22]. Jiho Choi et al. [23] demonstrated the epigenetic similarity of sex-matched Blastocyst-derived embryonic stem cells and gonad-derived embryonic germ cells and identify DUSP9 as a regulator of female-specific hypomethylation [23, 24]. Actin binding protein 1 B (POF1B) is highly and specifically expressed in polarised epithelial tissues [25]. Valeria Padovano et al. [26] found that POF1B plays a key role in organizing epithelial monolayers by regulating the actin cytoskeleton [26]. Shinsuke Katsuno et al. [27] performed immunostaining of intramural nerves in gallbladders samples from CBD patients and observed hypoplasia of intramural vascularity and perivascular plexuses [27]. Therefore, we selected WD repeat domain phosphoinositide-interacting protein 4 (WDR45) gene, which encodes a beta-propeller scaffold protein with a putative role in autophagy [28]. Pyrosequencing result show that WDR45 were hypermethylated in CBD patients. Based on the validation of candidate genes, Our study may provide useful information to explore the epigenetic pathology mechanism of the disease. Still, the relationship between these genes and CBD needs further research.

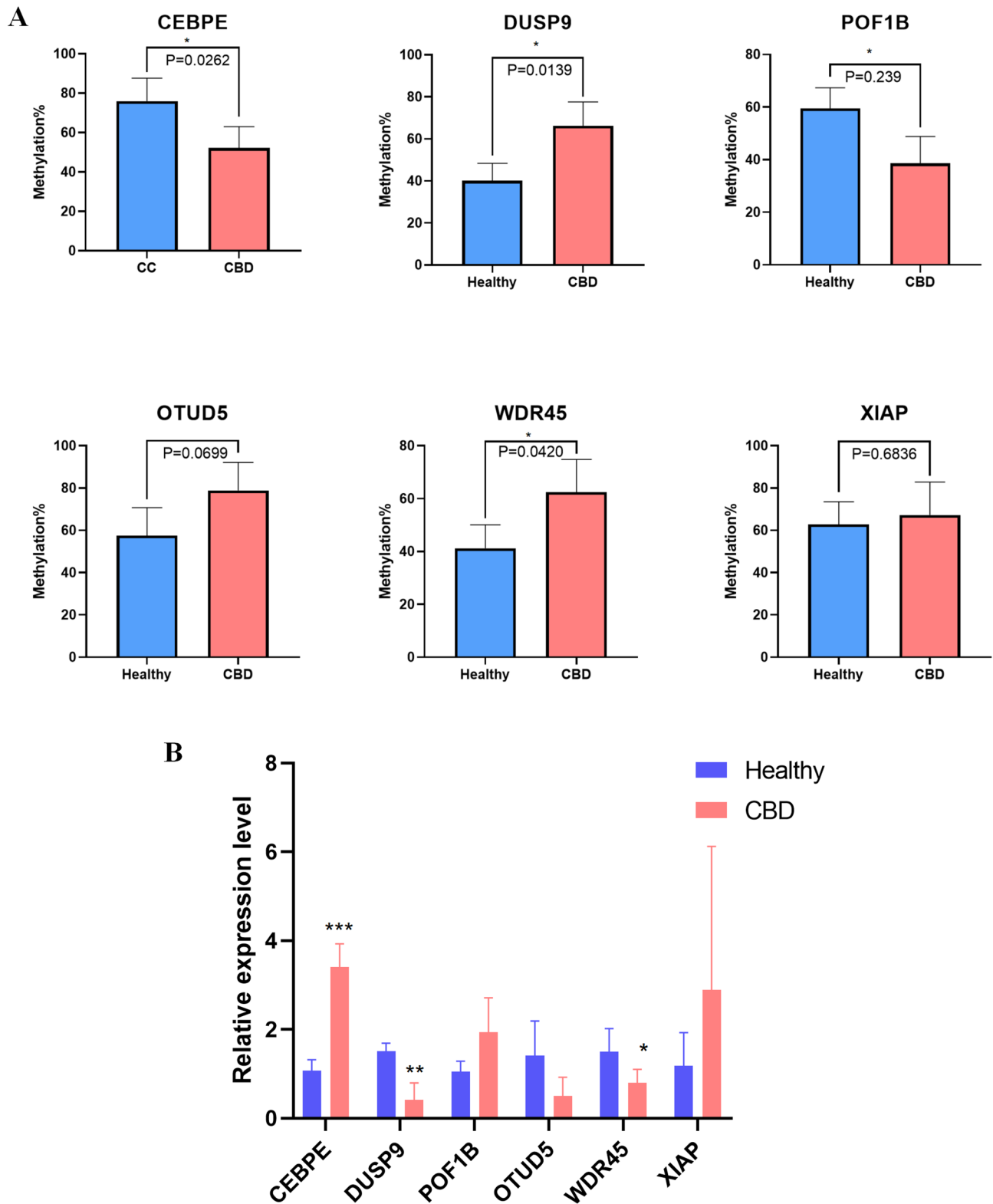


**Fig. 6** Validation of the results of the Illumina 850 K DNA methylation bead array analysis by pyrosequencing and qRT-PCR. **A** Differential analysis between Illumina 850 K array data and pyrosequencing. This section presents the concordance between the methylation levels determined by the Illumina 850 K Bead Array and those verified by pyrosequencing for select genes: CEBPE, DUSP9, POF1B, OTUD5, WDR45, and XIAP. The correlation coefficients and their statistical significance are depicted, indicating the reliability of the array data. **B** Gene Expression Validation by Quantitative Real-Time PCR (qRT-PCR): The expression levels of the aforementioned genes are confirmed through qRT-PCR, with results normalized to the housekeeping gene  $\beta$ -actin to account for variations in sample. \* $P < 0.05$ , \*\* $P < 0.01$ , \*\*\* $P < 0.001$

This study has several limitations. Despite the pioneering nature of our study in exploring the DNA methylation profiles in CBD, we are cognizant of its limitations, particularly the small sample size which restricts the generalizability of our findings. Our analysis indicates significant differential methylation in genes such as CEBPE, DUSP9, POF1B, and WDR45. Future research should aim to investigate the intricate relationships between methylation patterns, disease severity, and treatment outcomes to unravel the complex epigenetic mechanisms in CBD. Additionally, our study did not involve special handling or exclusion of sex chromosome data. This omission may lead to some bias in the interpretation of methylation levels, especially when considering mixed-gender samples. The potential for gender-related biases in the methylation patterns observed on sex chromosomes should be noted, and we recommend that future research considers the impact of sex chromosomes separately to better understand their role in CBD.

## Conclusion

In summary, this study provides the first genome-wide methylation landscape of congenital biliary dilatation in children. We identified widespread and significant alterations in DNA methylation patterns in the peripheral blood of CBD patients, implicating key genes and pathways, notably those involved in immune regulation like the T cell receptor signaling pathway. The successful validation of methylation and expression changes in genes such as CEBPE, DUSP9, POF1B, and WDR45 underscores their potential roles in CBD pathogenesis. Future studies with larger cohorts are warranted to confirm these findings and to explore the translational potential of these epigenetic markers for improving diagnosis and understanding the pathophysiology of CBD.

## Abbreviations

|       |   |
|-------|---|
| CBD   | Congenital biliary dilatation                           |
| DMR   | Differentially methylated region                        |
| CT    | Computed tomography                                     |
| MRI   | Magnetic resonance imaging                              |
| SBP   | Systolic blood pressure                                 |
| DBP   | Diastolic blood pressure                                |
| TG    | Triglyceride  |
| TC    | Total cholesterol                                       |
| ALT   | Alanine aminotransferase                                |
| TBil  | Total bilirubin   |
| GGT   | $\gamma$ -Glutamyl transferase                          |
| CEBPE | CCAAT/enhancer-binding protein epsilon                  |
| DUSP9 | Dual specificity protein phosphatase 9                  |
| POF1B | Actin binding protein 1 B                               |
| OTUD5 | OTU domain-containing protein 5                         |
| WDR45 | WD repeat domain phosphoinositide-interacting protein 4 |
| XIAP  | X-linked inhibitor of apoptosis                         |

## Supplementary Information

The online version contains supplementary material available at <https://doi.org/10.1186/s12920-025-02223-3>.

Additional file 1: Table S1. Illumina Human Methylation 850 K Beadchip Raw Data. Table S2. Primers of this study. Table S3. CBD-associated site differences in DNA methylation. Table S4. Differentially methylated positions of DMR

Additional file 2

## Acknowledgements

Not applicable.

## Authors' contributions

FQ conceived the study design and funding acquisition. WCY and ZYL recruited participants and prepared samples. WY and WCY conducted lab experiments, FQ and ZYL contributed to writing—original draft, FQ contributed to writing—review and editing. All authors contributed to the article and approved the submitted version. All authors read and approved the final manuscript.

## Funding

This study was supported by Shenzhen Science and Technology Program (JCYJ20230807093800002), Guangdong High-level Hospital Construction Fund Clinical Research Project of Shenzhen Children's Hospital (LCYJ2022074) and Sanming Project of Medicine in Shenzhen (SZSM202411010).

## Data availability

All relevant data, including the original sequencing data, are accessible both within the manuscript and its Additional files. The genome-wide methylation microarray data generated in this study have been deposited in the NCBI Gene Expression Omnibus (GEO) database under accession number GSE275555, and the data can be accessed at the following link: <https://www.ncbi.nlm.nih.gov/geo/query/acc.cgi?acc=GSE275555>. Additionally, the original contributions presented in this study are included in the Supplementary Material of the article.

## Declarations

### Ethics approval and consent to participate

In compliance with the State Drug Administration and the National Health and Wellness Commission's "Code for Quality Management of Drug Clinical Trials" (2020), "Code for Quality Management of Clinical Trials of Medical Devices" (2016), the Ministry of Health's "Biomedical Research Involving Humans Ethical Review Measures" (2016), the Declaration of Helsinki, and the CIOMS International Ethical Guidelines for Health-related Research Involving Humans, our study was conducted under rigorous ethical considerations. The Ethics Committee of Shen Zhen Children's Hospital (Approval No. 202002902) granted approval for the studies involving human participants. We ensured that informed consent was obtained from all study participants, or their legal guardians where applicable. Additionally, for any cadaver samples included in the study, we obtained consent from the next of kin, in accordance with the ethical standards set forth for research involving human subjects.

### Consent for publication

Not applicable.

### Competing interests

The authors declare no competing interests.

Received: 8 August 2024 / Accepted: 26 August 2025

Published online: 23 October 2025

## References

- Okada A, Hasegawa T, Oguchi Y, Nakamura T. Recent advances in pathophysiology and surgical treatment of congenital dilatation of the bile duct. *J Hepatobiliary Pancreat Surg.* 2002;9(3):342–51.
- Nederlandse Studiegroep voor Choledochus Cm, van den Eijnden MHA, de Kleine RHJ, de Blaauw I, Peeters P, Koot BPG, et al. Choledochal malformation in children: lessons learned from a Dutch National Study. *World J Surg.* 2017;41(10):2631–7.
- Atkinson JJ, Davenport M. Controversies in choledochal malformation. *S Afr Med J.* 2014;104(11):816–9.
- Wang DC, Liu ZP, Li ZH, Li DJ, Chen J, Zheng SG, et al. Surgical treatment of congenital biliary duct cyst. *BMC Gastroenterol.* 2012;12:29.
- Todani T, Watanabe Y, Toki A, Morotomi Y. Classification of congenital biliary cystic disease: special reference to type Ic and IVA cysts with primary ductal stricture. *J Hepatobiliary Pancreat Surg.* 2003;10(5):340–4.
- Minezaki S, Misawa T, Watanabe M, Takahashi H, Koenuma T, Kondo R, et al. A case with massive hemobilia long-term after internal drainage surgery for congenital biliary dilation. *Surg Case Rep.* 2021;7(1):157.
- Diao M, Li L, Cheng W. Congenital biliary dilatation may consist of 2 disease entities. *J Pediatr Surg.* 2011;46(8):1503–9.
- Mori H, Masahata K, Umeda S, Morine Y, Ishibashi H, Usui N, et al. Risk of carcinogenesis in the biliary epithelium of children with congenital biliary dilatation through epigenetic and genetic regulation. *Surg Today.* 2022;52(2):215–23.
- Meng H, Cao Y, Qin J, Song X, Zhang Q, Shi Y, et al. DNA methylation, its mediators and genome integrity. *Int J Biol Sci.* 2015;11(5):604–17.
- Mattei AL, Bailly N, Meissner A. DNA methylation: a historical perspective. *Trends Genet.* 2022;38(7):676–707.
- Dor Y, Cedar H. Principles of DNA methylation and their implications for biology and medicine. *Lancet.* 2018;392(10149):777–86.
- Kim H, Wang X, Jin P. Developing DNA methylation-based diagnostic biomarkers. *J Genet Genomics.* 2018;45(2):87–97.
- Udomsinprasert W, Kitkumthorn N, Mutirangura A, Chongsrisawat V, Poovorawan Y, Honsawek S. Global methylation, oxidative stress, and relative telomere length in biliary atresia patients. *Sci Rep.* 2016;6:26969.
- Aryee MJ, Jaffe AE, Corrada-Bravo H, Ladd-Acosta C, Feinberg AP, Hansen KD, et al. Minfi: a flexible and comprehensive Bioconductor package for the analysis of Infinium DNA methylation microarrays. *Bioinformatics.* 2014;30(10):1363–9.
- Wang D, Yan L, Hu Q, Sucheston LE, Higgins MJ, Ambrosone CB, et al. IMA: an R package for high-throughput analysis of Illumina's 450K Infinium methylation data. *Bioinformatics.* 2012;28(5):729–30.
- Teschendorff AE, Marabita F, Lechner M, Bartlett T, Tegner J, Gomez-Cabrero D, et al. A beta-mixture quantile normalization method for correcting probe design bias in Illumina Infinium 450 k DNA methylation data. *Bioinformatics.* 2013;29(2):189–96.
- Tian Y, Morris TJ, Webster AP, Yang Z, Beck S, Feber A, et al. ChAMP: updated methylation analysis pipeline for Illumina BeadChips. *Bioinformatics.* 2017;33(24):3982–4.
- Xie C, Mao X, Huang J, Ding Y, Wu J, Dong S, et al. KOBAS 2.0: a web server for annotation and identification of enriched pathways and diseases. *Nucleic Acids Res.* 2011;39(Web Server issue):W316–322.
- Okuma T, Hirata M, Yano F, Mori D, Kawaguchi H, Chung UI, et al. Regulation of mouse chondrocyte differentiation by CCAAT/enhancer-binding proteins. *Biomed Res.* 2015;36(1):21–9.
- Wada T, Akagi T. Role of the leucine zipper domain of CCAAT/enhancer binding protein-epsilon (C/EBPepsilon) in neutrophil-specific granule deficiency. *Crit Rev Immunol.* 2016;36(4):349–58.
- Musialik E, Bujko M, Kober P, Grygorowicz MA, Libura M, Przestrzelska M, et al. Comparison of promoter DNA methylation and expression levels of genes encoding CCAAT/enhancer binding proteins in AML patients. *Leuk Res.* 2014;38(7):850–6.
- Wu F, Lv T, Chen G, Ye H, Wu W, Li G, et al. Epigenetic silencing of DUSP9 induces the proliferation of human gastric cancer by activating JNK signaling. *Oncol Rep.* 2015;34(1):121–8.
- Choi J, Clement K, Huebner AJ, Webster J, Rose CM, Brumbaugh J, et al. DUSP9 Modulates DNA Hypomethylation in Female Mouse Pluripotent Stem Cells. *Cell Stem Cell.* 2017;20(5):706–19.
- Khoubai FZ, Grosset CF. DUSP9, a Dual-Specificity Phosphatase with a Key Role in Cell Biology and Human Diseases. *Int J Mol Sci.* 2021;22(21).
- Rizzolio F, Bione S, Villa A, Berti E, Cassetti A, Bulfone A, et al. Spatial and temporal expression of POF1B, a gene expressed in epithelia. *Gene Expr Patterns.* 2007;7(4):529–34.
- Padovano V, Lucibello I, Alari V, Della Mina P, Crespi A, Ferrari I, et al. The POF1B candidate gene for premature ovarian failure regulates epithelial polarity. *J Cell Sci.* 2011;124(Pt 19):3356–68.
- Katsuno S, Ando H, Watanabe Y, Harada T, Seo T, Kaneko K. Hypogenesis of intramural vascularity and perivascular plexuses of gallbladder in patients with congenital biliary dilatation. *J Hepatobiliary Pancreat Surg.* 2009;16(3):339–45.
- Zhao YG, Sun L, Miao G, Ji C, Zhao H, Sun H, et al. The autophagy gene Wdr45/Wipi4 regulates learning and memory function and axonal homeostasis. *Autophagy.* 2015;11(6):881–90.

## Publisher's Note

Springer Nature remains neutral with regard to jurisdictional claims in published maps and institutional affiliations.